	QO	QG	QH
Length [m]	3.5	2.0	1.6
Inner aperture [mm]	45	55	75
Tilt w.r.t.detect.axis[mrad]	-4	0	0
Gradient [T/m]	12	13	11
Average dipole field [T]	0.235	0.224	0.219
Average beam offset w.r.t magnet axis[mm]	7.7	29	32

Table 28: Requirements

8.13 Rev. 2–Lattice Superconducting Coils for QO, QG and QH

8.13.1 General

Various coil arrangements for the three magnets QO (downstream) and QG and QH (upstream) have been discussed, finally symmetric coils are proposed. Each magnet consists of a quadrupole coil with three layers and a single layer dipole coil. Eventually a skew dipole coil will be added.

8.13.2 Superconductor

A superconducting wire from a catalogue [1] has been used as a starting point. No checks on availability have been made so far. The wire parameters are:

- diameter (incl.insulation) is 0.9 mm (bare wire 0.85 mm)
- critical current at 4.2 K is 1272 A at $B = 2T$, 1046 A at $B = 3T$
- Cu/SC 1.34, 54 filaments with a filament diameter of $75\mu m$

8.13.3 Radial Coil Geometry

Each magnet has a quadrupole coil with 3 layers. The bare tube first gets an insulation layer of a GKG[2] tape, 50% overlapping, glued with Epoxy (thickness 0.5 mm). Then follows alternating a cable layer, an insulation layer of GKG with a thickness of 0.15 mm and an epoxy impregnated glass fiber bandage with a thickness of 0.2 mm, which tightens and secures the individual layers of the coil after curing.

8.13.4 Azimuthal Geometry

In order to obtain the gradient required and a good field quality, three quadrupole layers were necessary to approximate a $cos(2\theta)$-distribution. For the dipole coils one layer is sufficient for the field strength, but two spacers were added to improve the field quality. The parameters of the coils are summarized in tables 29,30. Fig 63 shows the geometry of the coil.

[1] Type OK54/1.34 from OUTOKUMPU Superconductors, Finland
[2] Glassfiber - Kapton - Glassfiber tape

	Q0	QG	QH
$R_{firstlayer}$ [mm] center of wire	54.95	64.95	84.95
$R_{secondlayer}$ [mm]	56.2	66.2	86.2
$R_{thirdlayer}$ [mm]	57.45	67.45	87.45
Turns (layer 1,2,3)	43, 32, 16	51, 38, 20	71, 48, 29
Coil angle [degree] first layer	0 - 40.35	0 - 39.69	0 - 28.71
Coil angle [degree] second layer	0 - 29.36	0 - 29.60	0 - 28.71
Coil angle [degree] third layer	0 - 14.36	0 - 16.82	0 - 17.10
Gradient/Current $[T/(m \cdot A)]$	0.03692	0.03229	0.02684
Contrib. of quadr. coil to dipole field [T]	0.093	0.373	0.352
Current	325	403	443

Table 29: : Quadrupole Coil

	Q0	QG	QH
R [mm] wire center	58.7	68.7	88.7
Turns	65	76	99
Coil angle [degree]	0 - 69.39	0 - 69.05	0 - 69.70
Spacer 1 Pos. [degree] missing turns	35.14 - 40.41	35.28 - 39.78	34.88 - 40.11
turns	6	6	9
Spacer2 [degree] missing turns	55.34 - 62.37	54.79 - 62.30	55.23 - 62.20
Turns	8	10	12
Field/Current [T/A]	0.000711	0.000715	0.000713
Current [A]	200	-209	-187
Contribution of dipole coil to dipole field [T]	0.142	-0.149	-0.133

Table 30: Dipole Coil

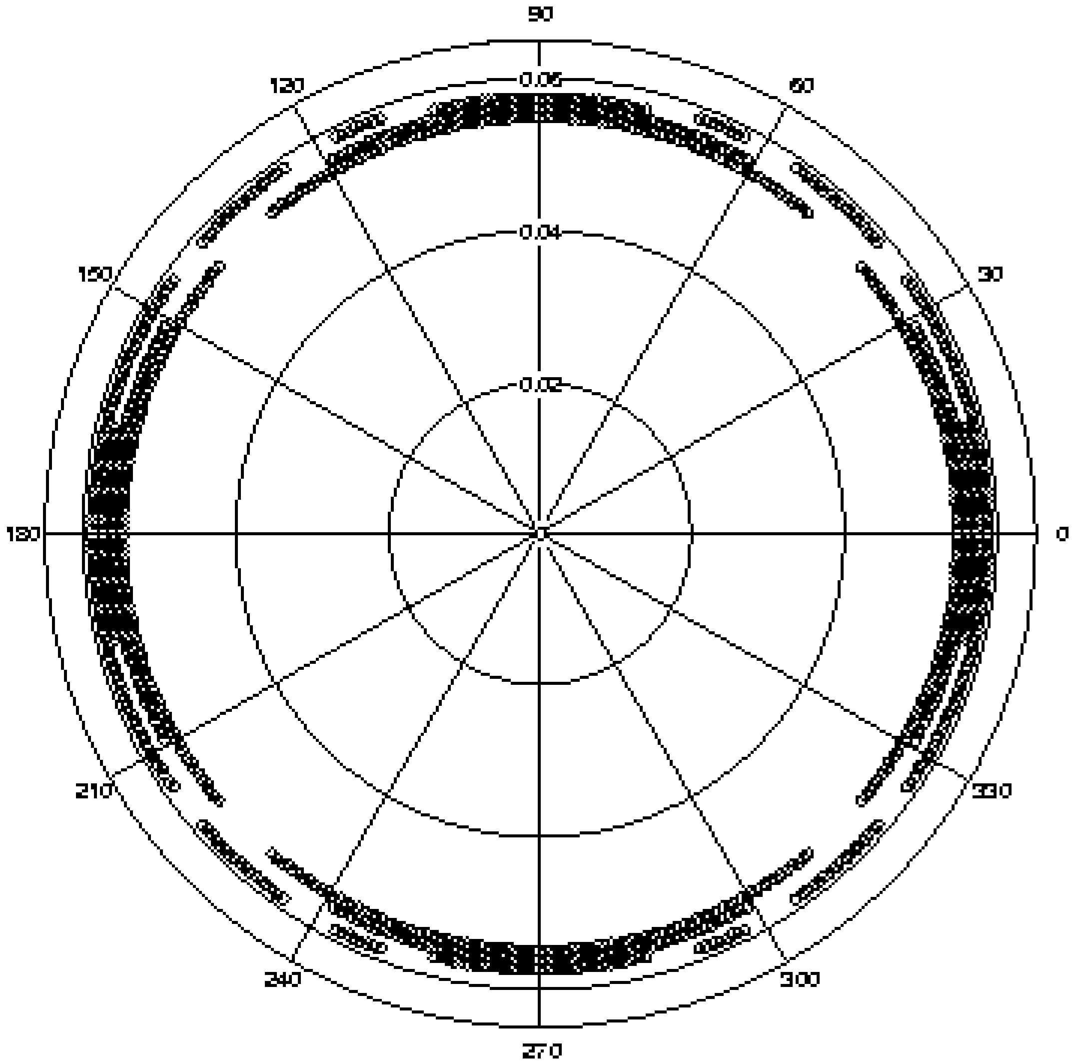

Figure 63: Coil Geometry

8.13.5 Currents

The current of the quadrupole coils are chosen to get the requested gradient. They differ considerable and cannot be powered by a common power supply. In the magnet QO the diple coil is needed to obtain the required bending field of $0.235T$, while in QG and QH an opposite field is needed to reduce the dipole component of the quadrupole field at the beam orbit.

The local field at the wires is about one tesla, the additional field of the solenoid magnet is $1.3T$. The critical current of the superconductor for theis field is about $1100A$ at $4.2K$. This gives a sufficient safety factor of about 2.5 for the quadrupole current and an even larger one for the dipole coil.

8.13.6 Field Quality

The radial and azimuthal component of the magnetic field inside the coil can be expressed by a Fourier series:

	Q0	QG	QH
order n	$b_n 10^4$	$b_n 10^4$	$b_n 10^4$
3	-1.6	+3.5	-1.5
4	-0.8	+3.4	-1.4
5	1.6	0.6	2.6
6	1.8	-0.7	2.6
7	0.5	-5.0	0.3
8	0.9	-8.5	-1.0
9	0.4	-8.1	-0.9
10	≤ 0.1	-5.6	-0.4
11		-3.0	-0.1
12		-1.2	≤ 0.1
13		-0.2	
14		0.3	
15		0.5	

Table 31: Multipole Coefficients

$$B_r(r,\Theta) = \sum_{n=1}^{\infty} B_{ref} \cdot \left(\frac{r}{r_0}\right)^{n-1} \cdot (-a_n \cdot cos(n \cdot \Theta) + b_n \cdot sin(n \cdot \Theta)) \tag{36}$$

$$B_\Theta(r,\Theta) = \sum_{n=1}^{\infty} B_{ref} \cdot \left(\frac{r}{r_0}\right)^{n-1} \cdot (a_n \cdot sin(n \cdot \Theta) + b_n \cdot cos(n \cdot \Theta)) \tag{37}$$

The multipole coefficients a_n and b_n are used as a measure of the field quality at the reference radius r_0 of $25mm$. They are normalized to quadrupole field B_{ref}. The required field quality in terms of multipole coefficients is $a_n < 0.0005$ and $b_n < 0.0005$. The magnets have been modeled in MATHCAD. Coil ends are not taken into account in the calculation. In order to take into account the curved beam path in the magnet, the multipoles are calculated at three different beam offsets with respect to the magnet center and are then averaged. Because of the up-down symmetry all a_n components are zero. The angles of the coils and the width and position of the spacers in the dipole coil strongly influence the field quality. They were optimized such that the multipoles get small. The multipoles of QO and QH are well within the acceptable range. This is partially due to canceling of opposite contributions from the dipole and the quadrupole coil. For QG the multipoles are close to 10^-3 and it will be difficult to obtain a further reduction by optimizing the coil geometry.

Fig 64 summarizes the field quality of the QO magnet.

8.13.7 Mechanical Accuracy

In the model the wire positions were randomly distorted applying a gaussion distribution in the radial and tin the azimuthal direction. For a radial error of $\pm 0.125mm$ and an azimuthal error of $\pm 0.2mm$ the multipoles change by about 0.01% to 0.2%, and in addition skew multipoles of this size appear.

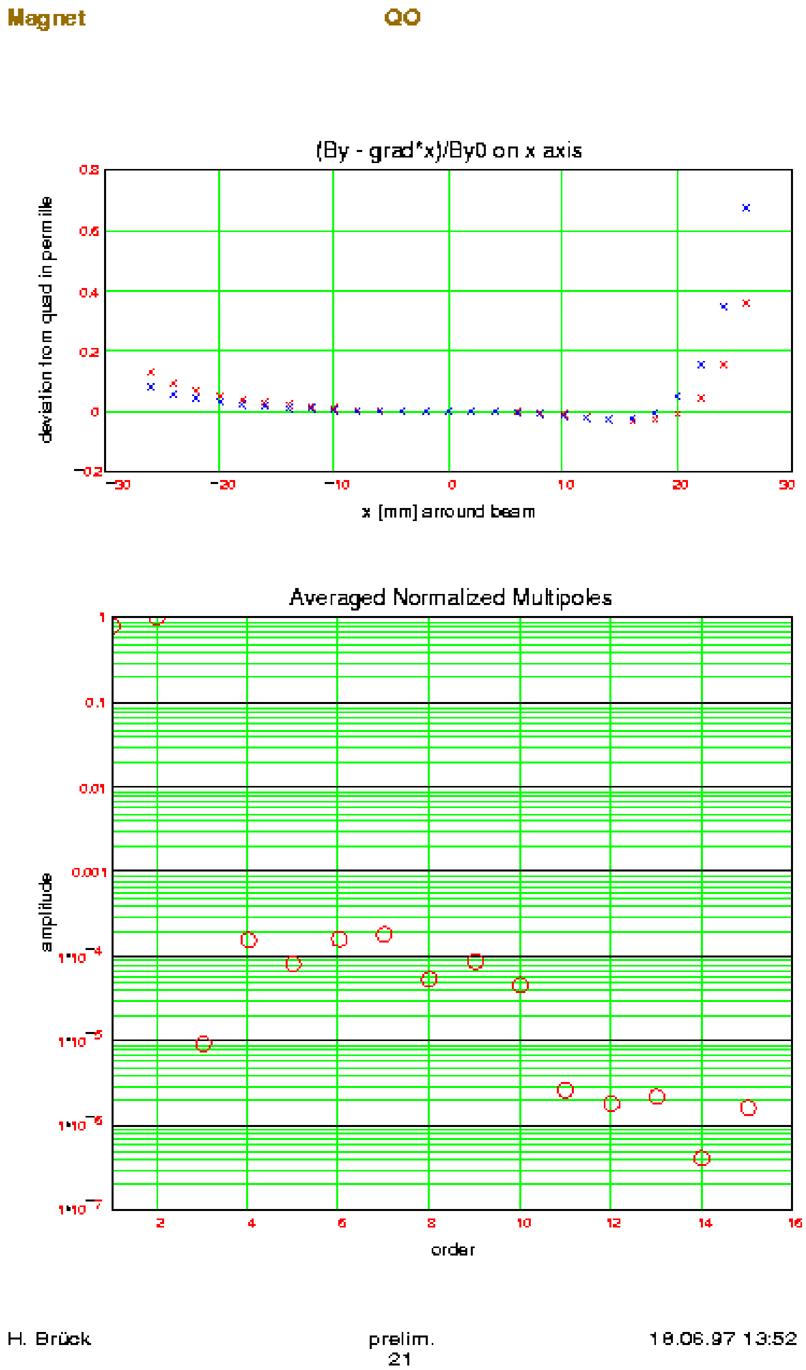

Figure 64: Field Quality

8.13.8 Cryostat Design

The structure of the cryostat consists of ellipitical and circular layers which are described one by one proceeding from inside to outside.

- **Beam Pipe:** The pipe has an elliptical shape and is made from stainless steel. It needs a $3mm$ wall thickness to be stable under $1bar$ athmospheric pressure. It is cooled down to $T = 70K$ and acts as thermal heat shield for the quadrupole coils which is operated at $4.6K$. The coolant supply (70K He gas) is connected to the beam pipe.
- **Insulation:** Five to ten layers of super-insulation are necessary in the insulating vacuum between beam-pipe/heat-shield and $4.6K$ part. The required thickness of the insulating vacuum $3mm$. The heat load on the $4.6K$ from thermal radiation of the $70K$ surface is less than one watt
- **Inner Helium Vessel Pipe:** It has a $3mm$ wall thickness. It needs a good "roundness" since is serves also as a mechanical support of the coils.
- **Coil:** The coil consists of insulated superconducting wire of $1mm$ thickness. It is wound on a glassfiber-epoxy mandrel which is glued to the inner pipe of the helium vessel. There is space for four layers including insulating layers. The magnetic forces will be controlled by glassfiber bandages. The cooling of the coil with liquide He of $4.6K$ is accomplished by a radially 2mm wide transport volume.
- **Outer Pipe of Helium Vessel** This pipe need a wall thickness of $2mm$. with these dimensions, the Helium vessel can hold an inner He pressure of $20bar$.
- **Outer Insulation Vacuum:** Between 30-40 layers of super insulations are necessary to shield the He vessel from radiation from the outer $300K$ surface. The insulating vacuum needs a thickness of $9mm$.
- **Vacuum Vessel:** It needs a wall of 3mm thick stainless steel. The outer diameter stays within $178mm$ including mechanical tolerances. In the case of the QO cryostat inside H1, the outer diameter is reduced at the positions of the welds at calorimeter-cryostat.

Fig 8.13.8 shows a cross section of the cryostat.

The He vessel has suuports made from glassfiber-epoxy blocks. The two Helium supply pipes inside the volume between the elliptical beam pipe and the circular Helium vessel have a diameter of $14mm$ and a wall thickness of $1mm$. There are made of stainless steel. One of the pipes also houses the superconducting cables of the electrical supply of the coils.

The zone in between the two downstream magnets which have very different apertures is proposed in the following way:
The Helium supply pipes have conflat flanges DN16. They can be connected and disconnected easily which is a necessary condition. The thermal contraction/expansion is compensated by a bellow. The electrical cables connections are contained in a box-shaped extension of the pipe. The installation and dismounting procedure is planned in the following way: The vacuum barrier to the outside has a removable sliding cylinder cover. The cylinder cover can be slided over the upstream small aperture magnet. The supply pipes are then accessible. At the downstream end of the downstream large aperture magnet are the current feed-throughs, the

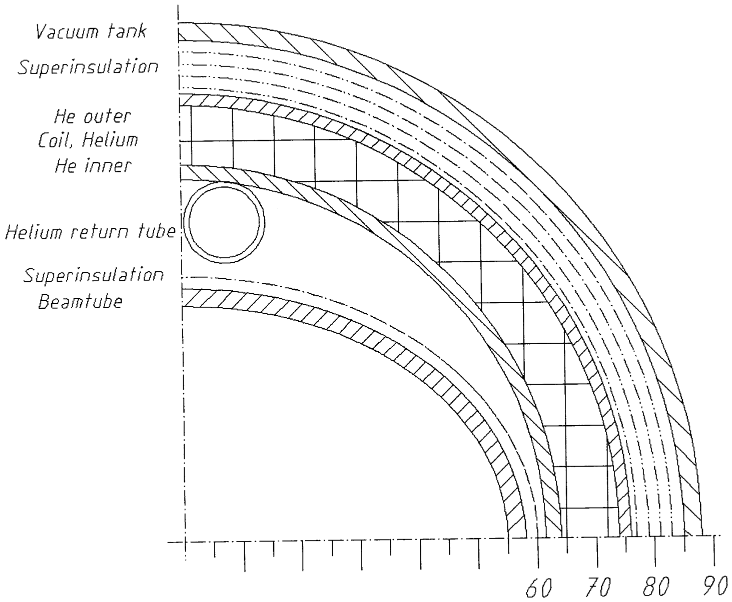

Figure 65: Cross section of the cryostat

cryogenic feedthroughs the pumping pipes for the insulating vacuum located. The long magnet on the upstream side of the detector is constructed in a similar way.

Fig 8.13.8 shows the downstream magnet connection, and Fig 8.13.8 shown in some detail the supplies feed-in at the downstream end.

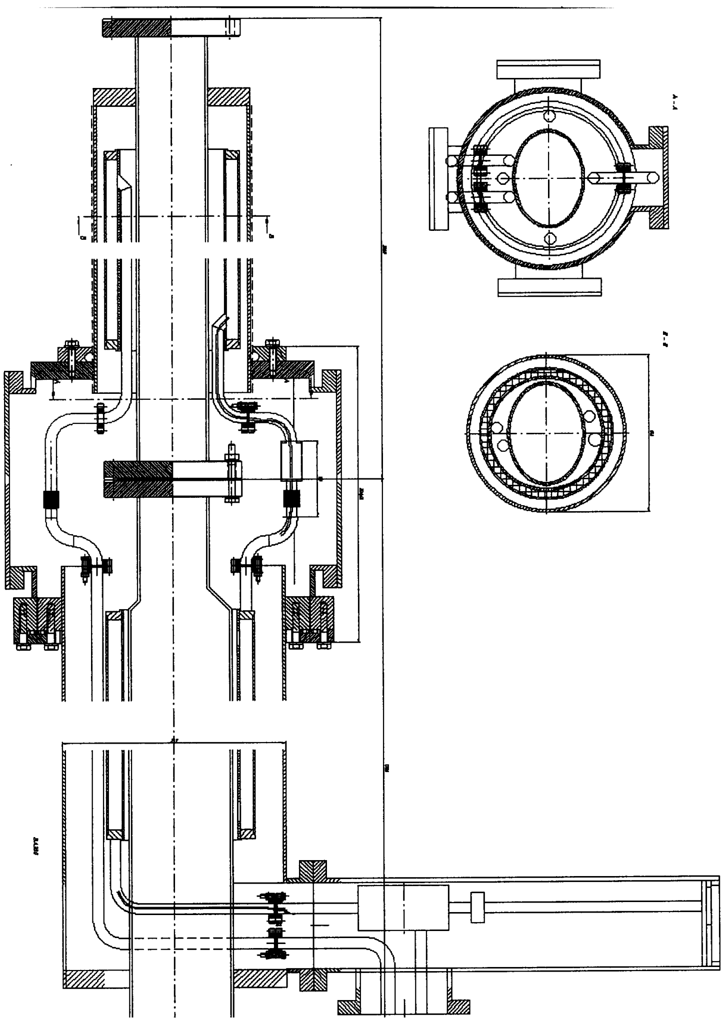

Figure 66: Connection between the downstream superconducting magnets inside the detector

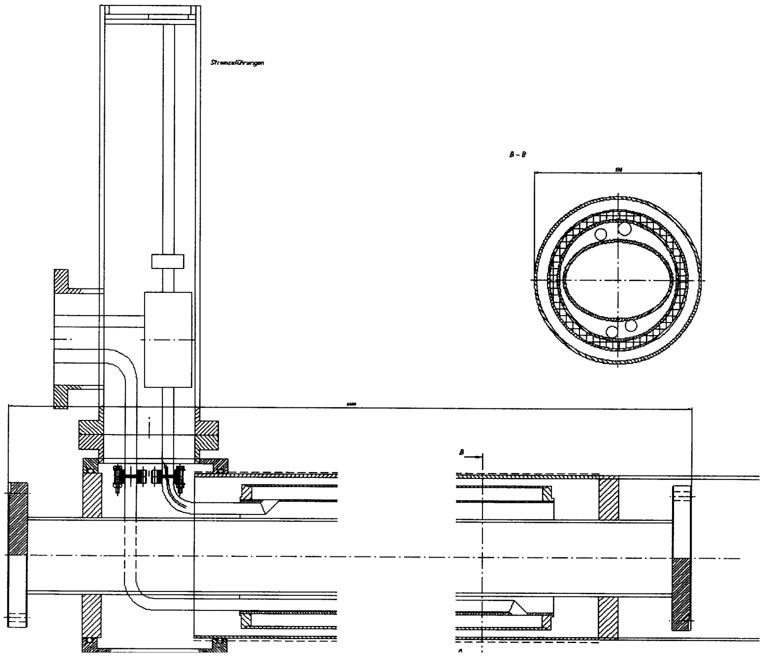

Figure 67: Detail of Connection of electrical and cryogenics supplies

8.13.9 Cooling Scheme

The superconducting coils will be cooled by helium between 4.4 and 4.6 K, whereas the beam pipe will be operated at a temperature level of about 70 K. Both circuits can be supplied from the existing HERA helium distribution system by establishing a branch from the helium hall supply boxes or from the helium distribution system of the H1 and ZEUS experiments. At each side of the IP there will be a supply box aside but nearest th the superconducting magnets: QO, QH and QG. QG and QH are cooled in series. In this supply box super critical, single phase helium is precooled in a subcooler to define the inlet temperature to the magnets, see Fig. 68. At the opposite side the helium is returned in a line which runs through the insulation vacuum between the coil cryostat and the beam pipe back to the precooler supply box. Before it enters the precooler container, it cools in addition the current leads of the quadrupole and dipole coils and is then expanded in a Joule Thomson valve to be reliquified into the precooler vessel. The 4.4 K inlet stream has to be adjusted with the corresponding inlet valve such that in steady state cooling conditions the level in the precooler remains constant within limits. For the cooling of the beam pipe helium is extracted at about 40 K from the high pressure (13 - 18 bar) shield cooling circuit of HERA. The supply line is thermally coupled to the beam pipe. At the end of the magnet(s) the helium returns through another tube, which also runs inside the insulation vacuum between the helium container of the coils and the beam pipe back to the 80 K shield return circuit of HERA. An actively cooled thermal outer shield around the coils has to be omitted, because of lack of radial space within the cryostat. Additional warm up lines are foreseen for both cooling circuits. Warm gas during cool down or from the gas cooled current leads is collected in the HERA quench gas collection line. The instrumentation like level sensors, heaters in the precooler, mass flow, pressure and temperature sensors as well as the necessary safety valves are not yet shown in the schematic drawing (Fig. 68). Also the connections to the existing helium system still have to be worked out.

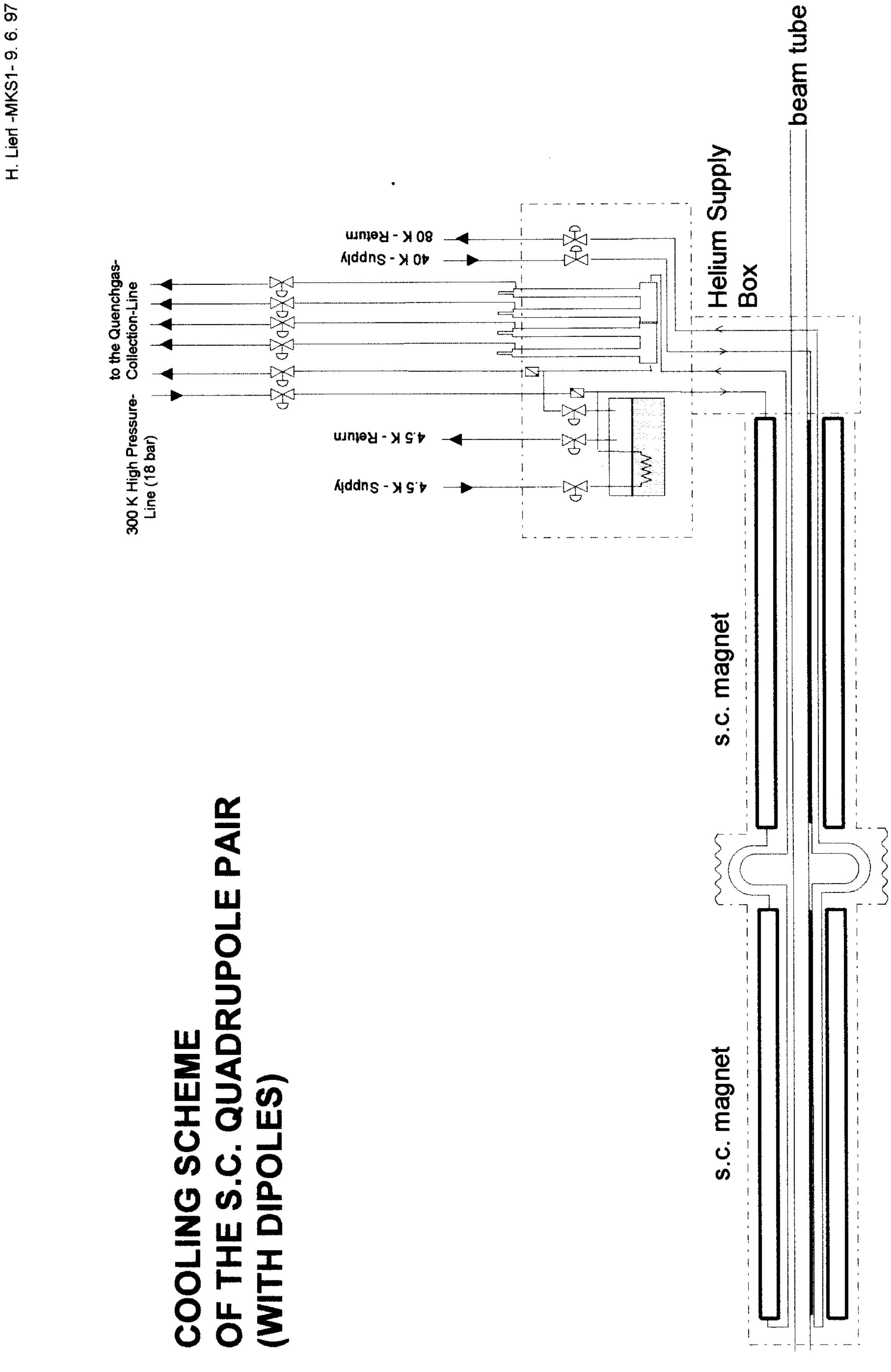

Figure 68: Cooling scheme of the superconducting magnets

9 Magnet Support Structure

9.1 Support of Magnets inside ZEUS

9.1.1 Analysis of Forces of Magnets and Components inside ZEUS

The interaction between the magnetic fields of the HERA magnets (QG and QH, **Rev1**) and the ZEUS magnet (solenoid and compensator) will result in additional forces on the support structures of both the HERA and the ZEUS magnets.

The magnets QH and QG have to fit into a cylinder along the z–axis with a radius $r < 10\,\mathrm{cm}$. We assume that the magnetic fields of the solenoid and compensator in this region are symmetric around the z–axis and are well described by:

$$B_z(r,z) = B_z(r=0,z) + \frac{B_z(r=100\,mm,z) - B_z(r=0,z)}{100} \times r[mm]$$

and

$$B_r(r,z) = \frac{B_r(r=100\,mm,z)}{100} \times r[mm]\,,$$

where the values $B_z(r=0,z)$,$B_z(r=100mm,z)$ and $B_r(r=100mm,z)$ are taken from the magnetic field map table calculated by F. Corriveau [1].

For further calculations we assume that the conductors of the air coils for the upgrade magnets have a point like cross–section. The applied force $\partial\vec{F}$ per length ∂l on such conductor with current $\vec{I}$ in a magnetic field $\vec{B}$ is given by:

$$\frac{\partial\vec{F}}{\partial l} = \vec{I} \times \vec{B},$$

with components:

$$\left(\frac{\partial\vec{F}}{\partial l}\right)_x = I_y \cdot B_z - I_z \cdot B_y\,,$$

$$\left(\frac{\partial\vec{F}}{\partial l}\right)_y = I_z \cdot B_x - I_x \cdot B_z\,,$$

$$\left(\frac{\partial\vec{F}}{\partial l}\right)_z = I_x \cdot B_y - I_y \cdot B_x$$

in the ZEUS–coordinate system.

The conductors of the combined–function magnet (QG), except at the head of the magnets, are parallel to the z–axis and $I_x = I_y = 0$. For this sections of the QG magnet the forces per conductor are:

$$\left(\frac{\partial\vec{F}}{\partial l}\right)_x = -I_z \cdot B_y = -I_z \cdot B_r \cdot \sin\varphi\,,$$

$$\left(\frac{\partial \vec{F}}{\partial l}\right)_y = I_z \cdot B_x = I_z \cdot B_r \cdot \cos\varphi \,,$$

$$\left(\frac{\partial \vec{F}}{\partial l}\right)_z = 0$$

and for n–conductors:

$$\left(\frac{\partial \vec{F}}{\partial l}\right)_x (z) = -\frac{B_r(r = 100mm, z)}{100} \sum_i^n (I_z)_i \cdot y_i \,[mm] \,,$$

$$\left(\frac{\partial \vec{F}}{\partial l}\right)_y (z) = \frac{B_r(r = 100mm, z)}{100} \sum_i^n (I_z)_i \cdot x_i \,[mm] \,.$$

Let us first consider the situation at the FCAL side. To get the total force acting on QH, except the coil heads, one has to integrate the last expression over z. Obviously, the x–component of the force will be zero, because QH is symmetrical in the $x - z$ plane. Assuming that QG positioned from $z = 1.6\,m$ to $z = 3.6\,m$, where $B_r(r = 100\,mm, z)$ drops down almost linearly from $\approx 420\,G$ to $\approx 54\,G$, the y–component of the force in case of electron operation in HERA is:

$$F_y\,[kN] = 0.486 \cdot I\,[kA] \,,$$

and applied at $z = 2.30\,m$, where I is the current per conductor in kA. In case of positron operation F_y changes sign.

Calculating the forces acting on the coil heads is much more complicated. Again because of symmetry arguments, only the F_y–component has to be taken in account and integrated over the conductor bends, but even this is not trivial. Thus the further calculations have to consider as an estimation.

It can be shown that the y–component of the force on the conductor bend of a half circuit with radius r in the $x - z$ plane is:

$$F_y = I \cdot r \cdot (\pi B_r - 2B_z) \approx -2 \cdot I \cdot r \cdot B_z,$$

where $B_z \gg B_r$ are the B_z and B_r components of the magnetic field of the ZEUS solenoid at the coil head. For $N = 24$ conductors :

$$F_y \approx -2 \cdot N \cdot I \cdot < r > \cdot B_z$$

or

$$F_y\,[kN] \approx -1.5 \cdot I\,[kA] \,,$$

if $< r >= 5\,cm$ and $B_z = 0.65\,T$. Again in case of e^+–beam in HERA, F_y will change sign.

In addition to these forces, the magnetic field produces a torque along the z–axis on QH

$$M_z\,[N \cdot m] = 12.8 \cdot I\,[kA]$$

as a result of the non–symmetry of the cross–section of the QG magnet.

The forces on the inner end of QG on RCAL side are identical to that on the FCAL side, of course all the values change their signs.

The forces would be much larger if the QH and QG magnets were located inside the ZEUS compensator. Due to the high return flux produced by the iron yoke at the end of the compensator, the value of $B_r(r = 100\,mm, z)$ goes up to almost $1\,T$. This would produce a large torque of $M_x \approx 18\ kN \cdot m$ which would destroy the internal support structure of the compensator.

The calculations will be repeated for the superconducting magnets (**Rev2**).

References

[1] F. Corriveau, ZEUS Note 90–046 (1990).

9.1.2 Description of Support Structure

The combined function magnets QG and QH (**Rev1**) will be mounted on a support structure, the so-called trough, on both sides of the interaction region. Both magnet will be mounted and adjusted such that their position cannot change with respect to the trough. In addition to the magnets, cables, cooling pipes and a laser alignment system will be inside the trough. All elements will be installed from the top. The trough will then be closed by a cover, which will be positioned by dowels and fixed by bolts.

The outer dimensions of the trough are defined by the available space inside the ZEUS forward and rear calorimeters of $200 \times 200 mm^2$ and a diameter of 240 mm inside the forward tracking detector, a 5 mm margin for clearance has to be subtracted on either side.

The support structure can be split between both magnets in order to simplify the installation. The joint has to be built such that the bending and torsion stiffness of the trough is not affected.

Inside the detector, the trough will be mounted on two bearings as shown in Fig. 69. The support inside the detector volume will be located between the forward tracking detector and the forward calorimeter, similar to the present support of the central beam pipe. On the other, side the trough will be mounted on the support structure of the following HERA magnets. The horizontal and vertical positions can be adjusted at both bearings when the detector is opened. Fig. 70 shows the support and adjustment inside the detector volume. The bending of the trough can be compensated remotely by an external moment, which will be applied at the outer bearing, as indicated in Fig. 71.

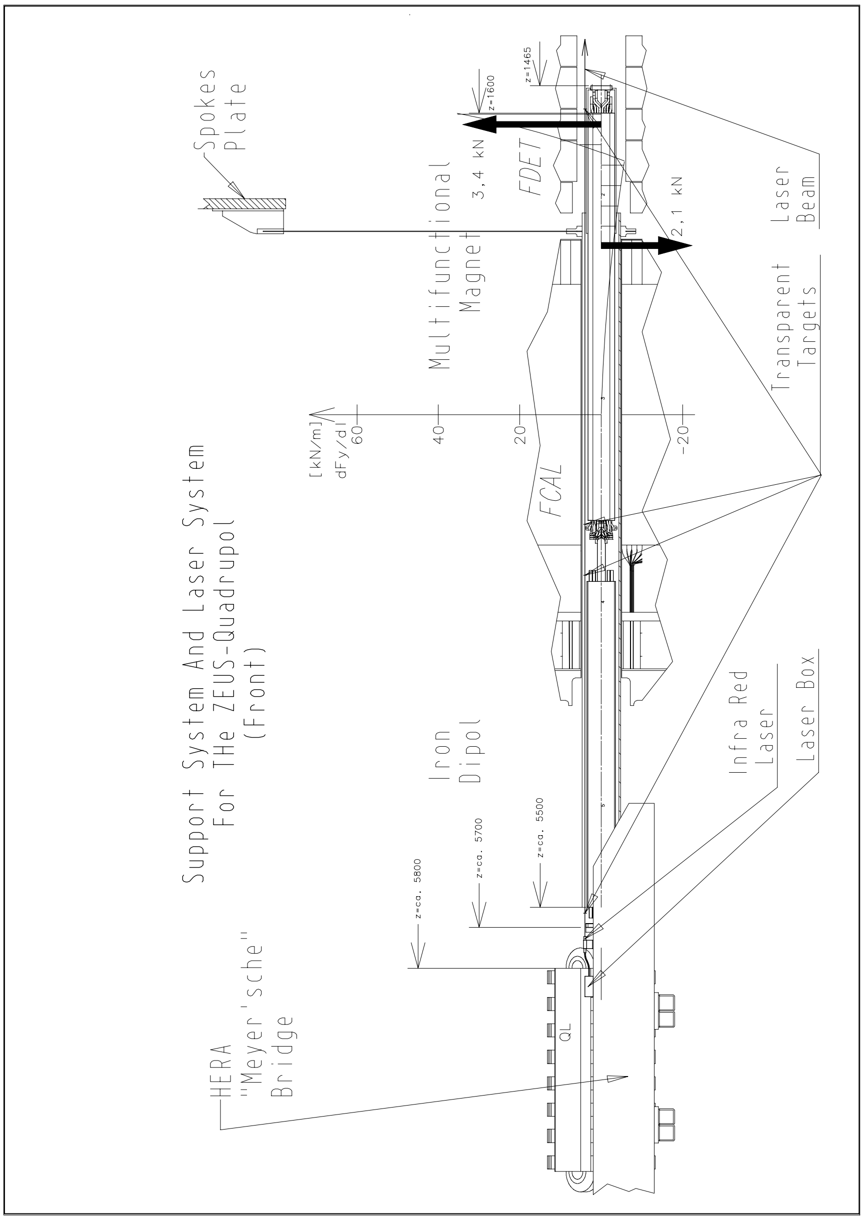

Figure 69: Trough with combined function magnets inside the ZEUS detector.

9.1.3 Specification of the Trough

Calculation of required Trough Cross Section The bending moment of inertia is given by

$$J_{x-x} = \sum_{j=1}^{n} F_j (y_j - \delta y)^2 + \sum_{j=1}^{n} J_j = 2944.16\, cm^4,$$

where F_j is a partial area of the total trough cross section, $y_j - \delta y$ the radius of inertia of the neutral line with respect to the cross section, J_j the moment of inertia of the partial area. The neutral line is calculated according to

$$\delta y = \frac{\sum_{j=1}^{n} F_j}{\sum_{j=1}^{n} S\ F_j y_j} = -2.95\, cm,$$

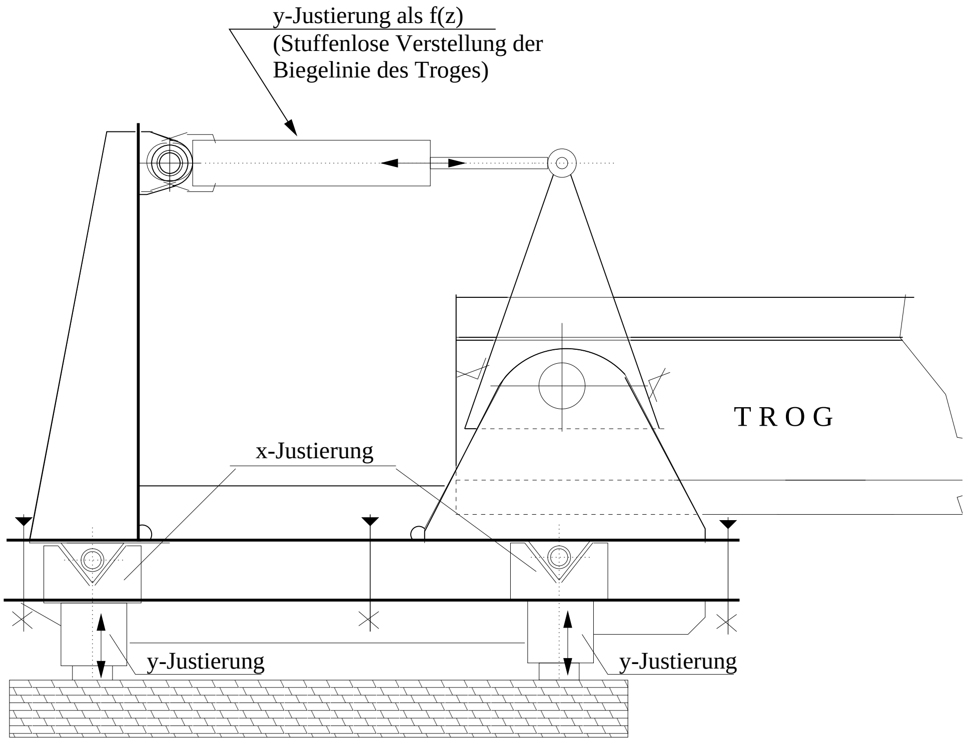

Figure 70: Sketch of the outer bearing with compensating mechanism.

where $S\,F_j y_j$ is the static moment of the partial area with respect to the symmetry axis of the trough cross section.

For $h_o = +y_{max} - \delta y = 12.45\,cm$ and $h_u = -y_{max} - \delta y = 6.55\,cm$, the bending moment of resistance is

$$W_o = \frac{J_{x-x}}{h_o} = 236.5\,cm^3 \qquad \text{and}$$

$$W_u = \frac{J_{x-x}}{h_u} = 449.5\,cm^3.$$

The torsion moment of inertia J_t and the torsion moment of resistance W_t are give by:

$$J_t = \frac{4F_m^2}{\oint \frac{ds}{\kappa}} = 3392.2\,cm^4 \text{and} W_t = 2F_m\kappa = 322.71\,cm^3,$$

where F_m is the trough cross section, ds a length element at the circumference of the trough cross section and κ the thickness of the length element.

Consideration of Loads Three main loads were calculated, all other cases were obtained by a superposition of the main loads. It was assumed that the magnets are made out of laminated sheets with no inherent stiffness. For cases 2 and 3, aquivalent single forces were used instead of the triangular stretch load, as calculated in the previous section. The different load cases are illustrated in the following figures and summarized in table 75.

Case 1: Weight of magnets The values in Fig. 72 are:
$l_s = 334\,cm$, $l_{\ddot{u}} = 56\,cm$, $a = 160\,cm$, $b = 174\,cm$, $c = 190\,cm$ and $d = 144\,cm$.
$q_1 = 3.843\,N/cm$, $q_2 = 15.625\,N/cm$ and $q_3 = 7.5\,N/cm$

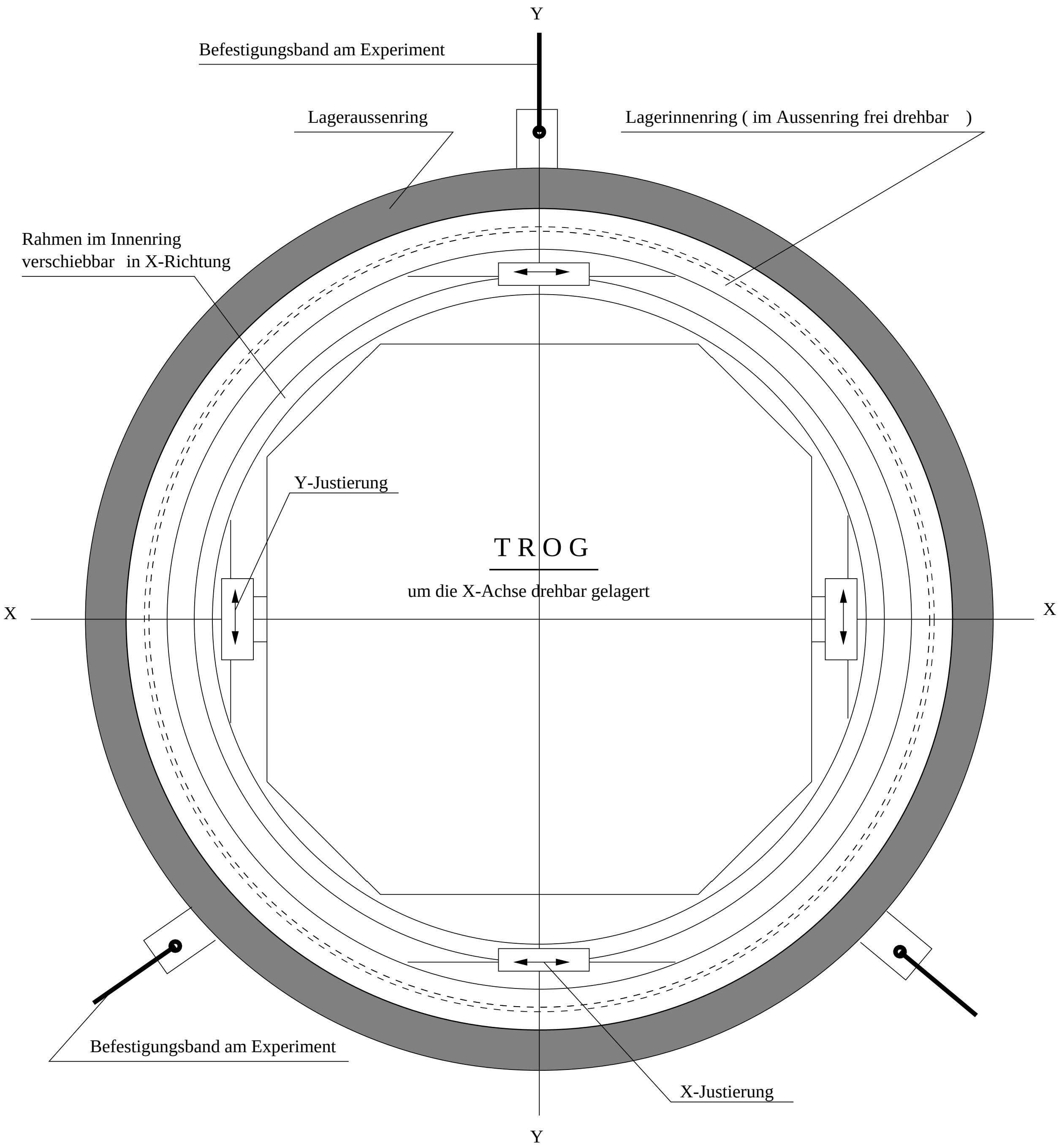

Figure 71: Sketch of trough support between forward calorimeter and tracking detector

Case 2: Magnetic forces – positron operation The values in Fig. 73 are: $a = 48\,cm,\ b = 28\,cm,\ c = 37\,cm,\ P_1 = 3.75 \cdot 10^{-1}\,kN,\ P_2 = 2.92 \cdot 10^{-1}\,kN,$ $P_3 = 5.68 \cdot 10^{-2}\,kN$ and $P_4 = -2.5\,kN$.

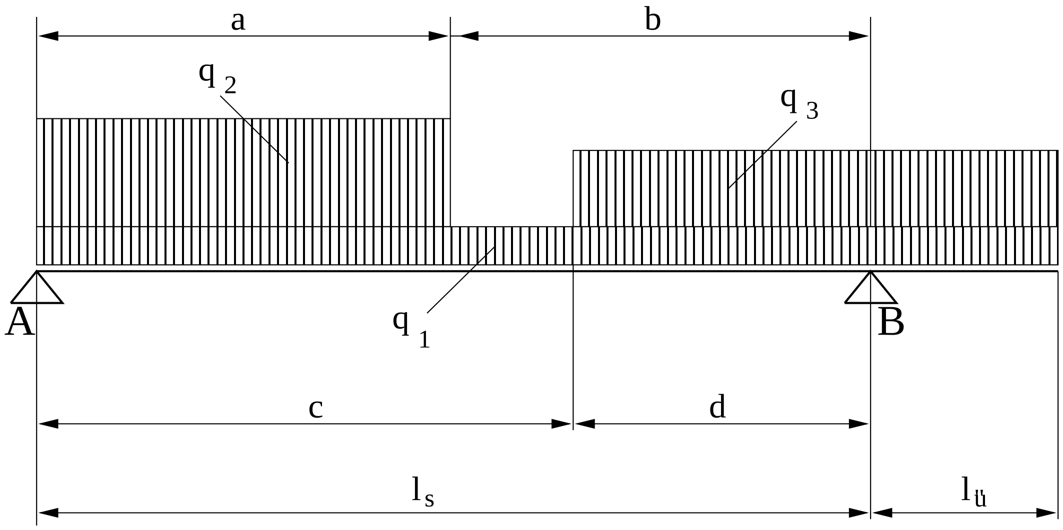

Figure 72: Loads due to mass of magnets and trough

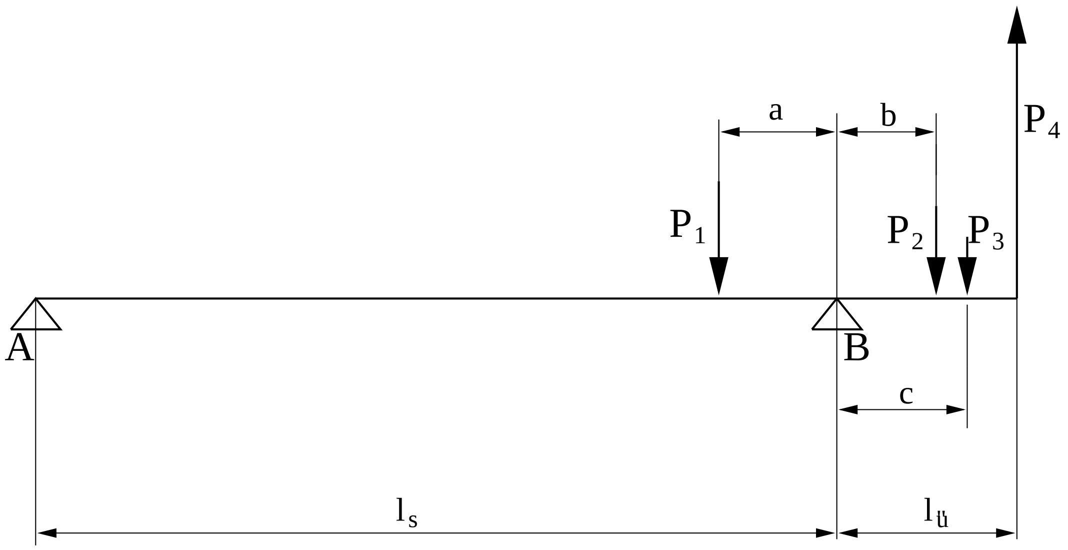

Figure 73: Loads due to magnetic fields during positron operation

Case 3: Magnetic forces – electron operation The force vectors are rotated by 180° with respect to positron operation. All absolute values are as in case 2.

Case 4 : Positron operation This case is a superposition of cases 1 and 2.

Case 5 : Positron operation This case is a superposition of cases 1 and 3.

Case 6 : Compensating moment at outer bearing The trough bending line is adjusted by applying an external moment at the outer bearing such that the position tolerances are fulfilled. The required compensating moment "KM" is $KM = M_A = -248.72\,kNcm$ for case 4. The resulting deflection at $l_S/2$ is the same as in case 4 but with opposite sign. Because of the clamping at bearing S, there will be a moment $M_B = 0$ at bearing B, and a rotation

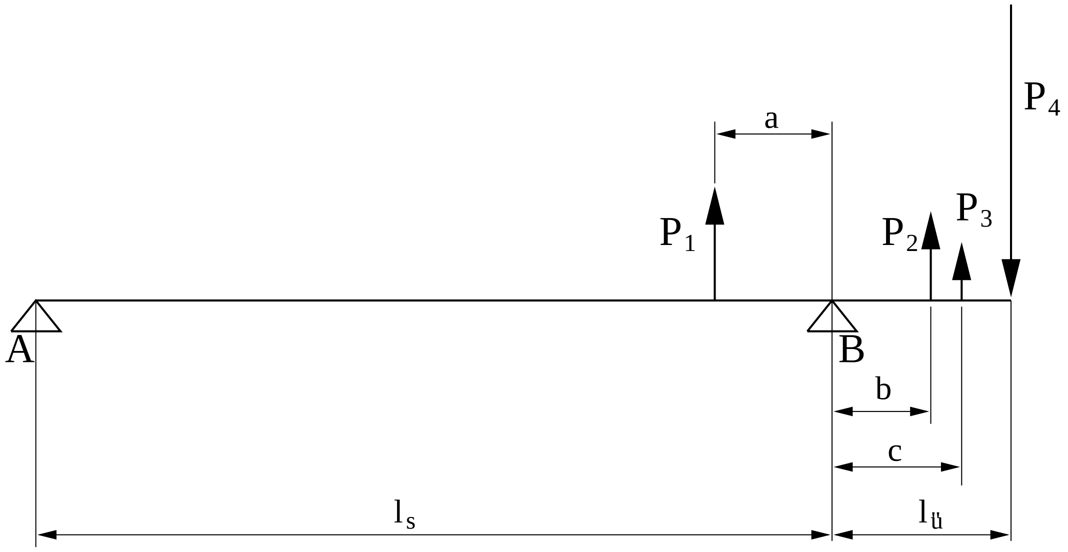

Figure 74: Loads due to magnetic fields during electron operation

of $\tan\phi_B = 2.2394 \cdot 10^{-4}$. The resulting deflection w (see Fig. 76 for a definition of w) at the unsupported side of the trough is $w = 3.154 \cdot 10^{-2}\,cm$.

Case 7 : Positron operation with compensating moment This case is a superposition of cases 4 and 6.

Case 8 : Quench of ZEUS Solenoid – Over compensating during positron operation This case is simulated by assuming that the magnetic forces P_1 and P_2 of case 2 act with opposite sign onto the clamped girder system. The resulting moments are obtained by superposition with case 7 and are summarized in table 75.

The support of the superconducting magnets (**Rev2**) will be similar to the support described in this section. The calculations will have to be repeated for the **Rev2** version.

Belastungsfall	Lager A (ausserhalb FCAL)		Lager B (vorm FDET)	
	Moment [cmkN]	Auflagerreaktion [kN]	Moment [cmkN]	Auflagerreaktion [kN]
Statisch durch die Masse von Trog und Magneten 1	0.0	2.743 ↑	-17.834	2.798 ↑
Magnetstrom eingeschaltet fur e+ Betrieb 2	0.0	0.445 ↑	+130.76	-1.686 ↓
Magnetstrom eingeschaltet fur e- Betrieb 3	0.0	-0.445 ↓	-130.76	1.686 ↑
e+ Betrieb 4 = 1 + 2	0.0	3.188 ↑	+112.93	1.112 ↑
e- Betrieb 5 = 1 + 3	0.0	2.298 ↑	-148.6	4.484 ↑
Kompensationsmoment am Auflager A 6	-248.72	0.745 ↑	0.0	-0.745 ↓
kompensierter e+ Betrieb 7 = 4 + 6	-248.72	3.933 ↑	+112.93	0.367 ↑
Quench im ZEUS-Solenoid 8	-239.15	3.475 ↑	-12.43	2.6 ↑

Figure 75: Bearing moments and forces

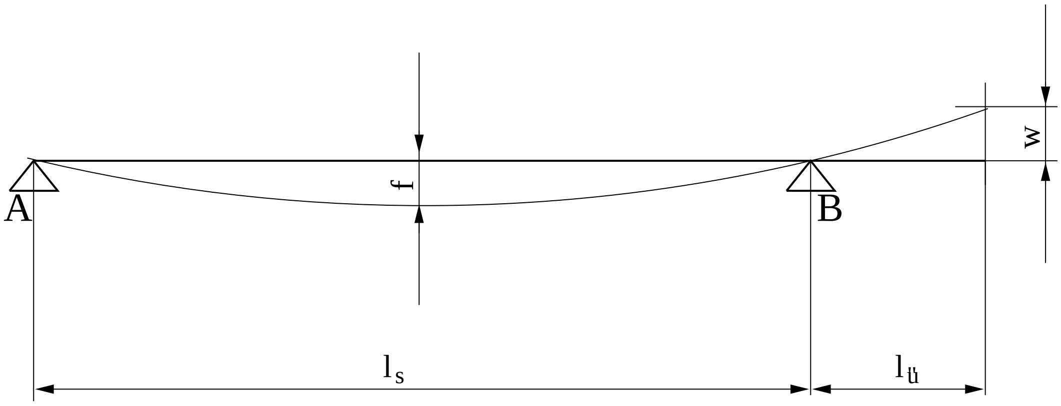

Lastfall	Eigenmasse	e^+- Betrieb	e^-- Betrieb
f [mm]	0.17	0.37	0.04
w [mm]	0.21	0.41	0.003

Figure 76: Deflection without compensating moment

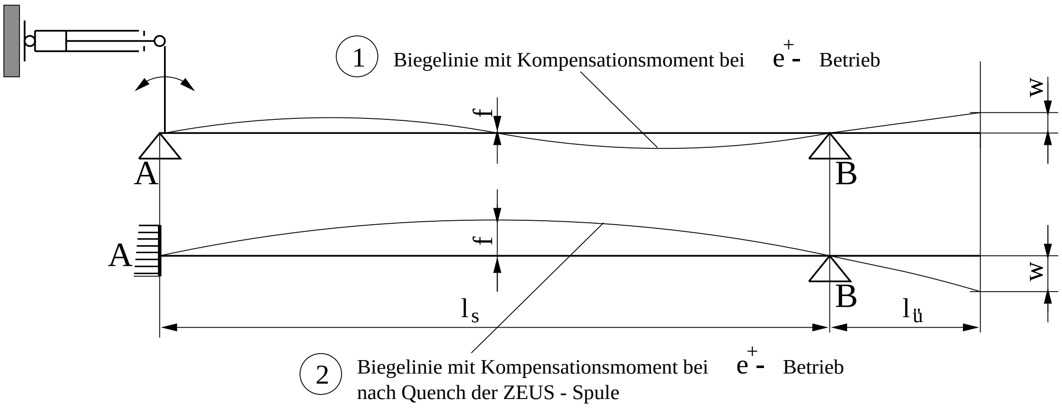

Betriebsart	f [mm]	w [mm]
1	0.00	0.095
2	0.188	0.15

Figure 77: Deflection with compensating moment

9.1.4 Installation Procedure

The installation procedure describes the work necessary in order to remove the present HERA magnets, collimators and beam pipes at the interaction region, and the installation of the new HERA components. Some of the items, which do not require crane operation can be done in parallel. The necessary length of the shut down, without any additional work on the detector, is estimated to about 3 months.

The procedure will be very similar in case of major repair of a magnet, the beam pipe or maintenance of the central tracking detectors (CTD, FDET, RTD, SiVXD), except for the items marked by a $\star$ (removal of the compensator and upstream HERA machine elements), which are only necessary for the first installation.

Work description	time estimate
Open yoke	1/2 d
Uncable F/RCAL, F/RHES, F/RPRES	10 d
Install F/RCAL extension rails	5 d
Move F/RCAL to extension rails	1 d
Install front and rear support frames	2 d
Remove forward beam pipe and C3/C4 collimators	1 d
Install FDET rails	1 d
Survey and adjust FDET rails	2 d
Uncable FDET	1 d
Install FDET windmill	1 d
Remove front N_2 shield	1/2 d
Remove FDET	1 d
Remove BPC and C5 counter	1/2 d
Remove central beam pipe	1 d
$\star$ Modify cryo tower	10 d
$\star$ Remove compensator	10 d
$\star$ Remove FMUON concrete shielding	1 d
$\star$ Open FMUON toroid	1/2 d
$\star$ Remove HERA magnets with beam pipes and collimators	2 d
$\star$ Remove or modify magnet support girder (bridge)	$\geq$ 2 d
$\star$ Install new magnet support girder (bridge)	2 d
$\star$ Install QI and QJ magnets with beam pipes	2 d
Install central beam pipe with vertex detector (temporary support)	1 d
Connect and check out vertex detector	5 d
Install rear (SR) QG, QH magnets inside support trough	1 d
Connect central beam pipe to beam pipe of QG magnet	1/2 d
Install forward (SL) QG magnet (temporary support)	1 d
Connect central beam pipe to beam pipe of QG magnet	1/2 d
Install FDET	1 d

Connect and check out FDET	3 d
Close front N_2 shield, leak test	1 d
Remove FDET windmill and rails	1 d
Install forward (SL) QH magnet	1 d
Survey and adjust FDET	2 d
Connect beam pipes, leak test	2 d
Connect magnets (power, cooling)	2 d
Check out magnets	1 d
Survey and align magnets and beam pipe	3 d
Remove front and rear support frames	1 d
Move F/RCAL from extension rails	1 d
Remove F/RCAL extension rails	5 d
Connect and check out F/RCAL, F/RHES, F/RPRES	20 d
$\star$ Close FMUON toroid	1 d
$\star$ Install FMUON concrete shielding	1 d
Close yoke	1/2 d

Most of the installation procedure remains unchanged when superconducting magnets are used instead of normal conducting magnets. The main difference is, that there will only be one superconducting magnet in the forward region (QO), which is about 4 m long. The forward tracking detector (FDET) and the QO magnet will have to be installed at the same time, because of space limitations. This requires a more complicated installation fixture. Of course, modifications of the cryo system are needed in case of superconducting magnets.

9.2 Support of Magnets inside H1

9.2.1 Analysis of Forces of Magnets and Components inside H1

Two types of forces have to be considered, which have to be supported by the H1 structures.

- The weight of the combined function magnets are assumed to be 2.0 kN per unit.
- The magnetic forces will vary with the excitation of the magnets
- The forces reverse their direction when switching from electrons to positrons. Therefore this report does not distinguish between the two possible directions of the magnetic forces.

The **forward QG magnet** is entirely within the main H1 field. Thus the forces on the two heads are symmetric, pointing into opposite directions at the two magnet heads. The current leads in the heads are assembled with an angle of 22^o with respect to the horizontal plane. Therefore the magnetic forces are pointing at an angle with respect to the vertical direction. Here we consider only the components parallel or antiparallel to the gravitational force, because the horizontal components above and below the median plane cancel to first order.

The vertical component of the magnetic forces on the ends are about 2.8 kN on each head assuming the following parameters:

- 1.15 T longitudinal field for the H1 magnet
- 1825 A current
- 6 cm for the average length of the magnet head.

The **backward QG magnet** has its inner head in the H1 main field but its outer end is positioned in the end-cap hole. The inner head will thus be exposed to also 2.8 kN. The outer one inside the end-cap receives a force of 1.4 kN due to the radial components of the H1 field. Also in this case the forces on the inner and outer heads will have opposite directions.

These forces are transferred via spokes wheels to the inner walls of the liquid Argon vessel resulting in a tolerable deformation of the structure. Details on the additional load introduced into the tank will be studied by finite element calculations.

9.2.2 Installation Procedure

For the long term operation of the high luminosity scheme it is not sufficient to only develop a scheme for the first installation. All components in the center of H1 have to remain accessible for repairs and later improvements. This access has to be non destructive and it has to be possible to complete it within a reasonable time of a few weeks at most. If the access problem is solved, it represents at the same time a viable scheme for the installation in the first place. Therefore this report will concentrate on describing the access procedure.

As a starting point the H1 experiment is supposed to be located in the beam position and access is required to the central part without moving H1 out of the interaction zone. The latter constraint is imposed in order to avoid the additional work of disconnecting the cryogenic systems for the superconducting solenoid and the liquid Argon calorimeter, which would introduce an unacceptable time delay.

For an access, the following steps have to be performed:

1. The iron yoke has to be opened by moving the North and the South shells into their parking position. This is a standard procedure, which is being done routinely.
2. The forward muon system has to be opened. Also a standard procedure.
3. The shielding wall across the forward muon system has to be removed. This is not a routine operation, but technically simple.
4. The first HERA machine elements, which are mounted on a common support in the forward direction, have to be removed. This is a simple crane operation.
5. Support structures and bridges have to be installed at beam level on the forward and backward faces of the detector to provide a working platform.
6. The second mini beta magnet (QH), which takes the space now occupied by the compensating solenoid, has to be lowered to the floor level to give room for the SPACAL to be pushed further back up to the HERA magnets mounted in the tunnel. In addition the backward drift chamber (BDC) has to be removed.

7. The backward detectors specifically the SPACAL calorimeter and some smaller units have to be rolled out of the solenoid, which is connected with major uncabeling work. This operation has been done every shut down so far.

8. **At this point the removal of the central beam pipe with the interaction magnets and Silicon trackers can start.**

9. The beam pipe forming one unit together with the interaction magnets is pushed from the +z side (forward direction) through the experiment and whenever a segment appears outside the central tracker, flanges are opened and the segments are moved out. This is the most critical part of the whole operation. The pushing procedure has been applied before, when H1 installed beam pipes and all tools were available. This time, however, the additional weight of the magnets has to be considered and a more advanced rolling system has to be designed.

The above procedure describes the access to the central beam pipe with the interaction magnets. For reinstallation the scheme is reversed. Different submodules are flanged together at the +z side and then pushed through H1 to the -z side.

The time estimated for a complete cycle with opening and closing the experiment is estimated to take about 8 weeks assuming 8 hours working days and 5 days per week. Between 2 and 3 weeks are needed for opening, and at least 5 weeks for closing, recabelling and testing.

In case access is required to the forward trackers or the central drift chambers, H1 has to be moved to the parking position. There essentially the same scheme will be pursued with the only difference that some of the operations are easier because of the better accessibility. The procedure described above assumes warm magnets in the interaction region. For superconducting coils we may follow essentially the same route except that additional time will be required for warming up and cool down. Disconnecting the cryo lines will not present a technical problem, because experience exists in H1 from disconnecting the main solenoid from the Helium supply. Also the extra time required is negligible compared with the total length down time needed for the complete operation.

10 Vacuum System

10.1 Specification of the Vacuum System in the IR

The background rate in the detector and the first level trigger rate of the data acquisition are determined by the beam conditions and by interactions of the electron and proton beams with the residual gas inside the vacuum system.

A residual gas pressure of $\lesssim 10^{-9}$ mbar is required at the interaction region and upstream of the proton beam for good running conditions. The pressure in the common vacuum system is mainly determined by the desorption induced by synchrotron radiation, thermal desorption, the available pumping speed and the conductance of the vacuum chambers. Thermal desorption due to higher order mode losses of the electron beam are small, provided there is adequate cooling of the vacuum chambers.